

PAPER • OPEN ACCESS

## The influence of carbon counter electrode composition on the performance of monolithic dye-sensitized solar cells

To cite this article: F Arif *et al* 2019 *J. Phys.: Conf. Ser.* **1191** 012021

View the [article online](#) for updates and enhancements.

### You may also like

- [Nanostructured perovskite oxides for dye-sensitized solar cells](#)  
Md Sariful Sheikh, Anurag Roy, Alo Dutta et al.
- [Understanding of the chopping frequency effect on IPCE measurements for dye-sensitized solar cells: from the viewpoint of electron transport and extinction spectrum](#)  
Guogang Xue, Xirui Yu, Tao Yu et al.
- [A review on ZnO nanostructured materials: energy, environmental and biological applications](#)  
J Theerthagiri, Sunitha Salla, R A Senthil et al.



**ECS**  
The  
Electrochemical  
Society  
Advancing solid state &  
electrochemical science & technology

**DISCOVER**  
how sustainability  
intersects with  
electrochemistry & solid  
state science research

# The influence of carbon counter electrode composition on the performance of monolithic dye-sensitized solar cells

F Arif<sup>1</sup>, N M Nursam<sup>2,\*</sup>, N Prastomo<sup>1</sup>, Shobih<sup>2</sup>

<sup>1</sup>Department of Physics Engineering, Faculty of Engineering, Surya University, Jl. Boulevard Gading Serpong, Tangerang, Banten 15810

<sup>2</sup>Research Center for Electronics and Telecommunication – Indonesian Institute of Sciences, Building 20 level 4 Kampus LIPI Jl. Sangkuriang, Cisit, Bandung 40135, Indonesia

\*Email: natalita.maulani.nursam@lipi.go.id

**Abstract.** In this research, the influence of carbon composition on the physical and electrical characteristics of the counter electrode and the performance of monolithic dye-sensitized solar cell (DSSC) was investigated. Screen printing method was used due to its excellence such as simple fabrication process at mass production. Physical and electrical characterization of the counter electrode layer were characterized by scanning electron microscopy (SEM), X-ray diffraction (XRD) analysis, gas sorption using Brunauer-Emmett-Teller (BET) method, and four-point probe measurement. Meanwhile, the DSSC performance was characterized using current-voltage (I-V) and incident photon-to-current efficiency (IPCE) measurement system. It is found that the carbon composition affects the physical and electrical characteristics of the counter electrode, such as the porosity, crystallinity, BET surface area, and micro-sized agglomeration. However, relatively similar conductivity values are obtained regardless of the carbon composition. The results show that the composition of graphite and active carbon with a ratio of 1:4 as a counter electrode material produced a porous layer with approximately 3.32  $\mu\text{m}$  of agglomerates and conductivity with a sheet resistance value of 11.60  $\Omega/\text{sq}$  that overall can improve the performance of the monolithic DSSC. The highest efficiency obtained is 1.52% and the highest QE value is 32% at the absorption area of  $\text{TiO}_2$ , with  $V_{\text{oc}}$ ,  $I_{\text{sc}}$  and  $P_{\text{max}}$  value of 0.63 V, 1.19 mA and 0.91 mW, respectively.

## 1. Introduction

A typical dye sensitized solar cell (DSSC) with sandwich structure consists of two electrodes, namely the working electrode and the counter electrode. Both of these electrodes are made of glass substrate coated with transparent conducting oxide (TCO) that is relatively expensive. As much as 80% the cost of DSSC solar cell fabrication is only used for the cost of fluorine-doped tin oxide (FTO) substrate, which is one of the most used types of TCO [1]. Therefore, researchers sought to reduce the cost of fabrication by modifying the configuration of the DSSC sandwich model into a monolithic structure by using only one FTO glass substrate. The monolithic DSSC consists of several components: photoanode, spacer/scattering layer and counter electrode coated on a conductive glass substrate [2].

Counter electrode in DSSC serves as a cathode that has several functions including as a catalyst to accelerate the redox reactions ( $\text{I}_3^-/\text{I}^-$ ), as the collector current to the external circuit, as well as electrolyte transport pathways and  $\text{ZrO}_2$  layers toward the dye/ $\text{TiO}_2$  [2]. Some of the criteria of an



ideal counter electrode that is able to improve the performance of monolithic DSSC are having low resistance, high surface area, mesoporous, and good mechanical integrity [3].

The material that is often used as a counter electrode in the sandwich model DSSC is platinum (Pt) because it has high catalyst activity and excellent stability [4]. In addition, by using platinum as a counter electrode, a sandwich type DSSC has been reported to obtain an efficiency of more than 12% [3]. However, Pt has limited availability and thus has a relatively expensive price. Carbon is an abundant material on earth and can be found almost everywhere. Carbon has high catalyst activity, porous, corrosion-resistant, high surface area, and is a low cost material [3].

Graphite is one type of carbon material that is often used as a counter electrode of sandwich model DSSC because it has a high electrical conductivity. However, graphite has a large particle size so the surface area is low [1]. This can inhibit reduction of  $I_3^-$  to  $I^-$  because the size of large graphite particles has fewer edge planes, in which the charge transfer resistance ( $R_{CT}$ ) is also high. The high  $R_{CT}$  influences the fill factor (FF) so the resulting efficiency is low [5]. In addition, large graphite particle sizes may cause between the particle relationships inadequate to produce high conductivity [1]. Therefore, the structure of the graphite material is preferably modified to add the number of edge plane and strengthen the relationship between the particles [6].

In the previous study, graphite has been combined with other carbon materials as counter electrode [7]. Combining graphite with amorphous carbon can be used to improve the performance of monolithic DSSC [8]. The amorphous carbon material can strengthen the bonding between graphite particles and also increase the number of edge planes in graphite material so that the conductivity and catalyst activity in the counter electrode increases, thus the electrolyte transfer rate to the spacer layer and photoanode also increases. Activated carbon with a particle size of 1-10  $\mu\text{m}$  has also succeeded in increasing the counter electrode conductivity in the sandwich-type DSSC [9]. This indicates that active carbon can potentially combined with graphite material as counter electrode in monolithic DSSC. Until now there has been no comparison between composition of graphite with nano-sized amorphous carbon, as well as graphite with micro-sized activated carbon. When synthesizing composite materials, there is an important thing that needs to be considered, namely ratio. The ratio may affect the overall performance of DSSC, wherein an optimum performance can be obtained with the right ratio [10]. Thus, the effect of carbon counter electrode composition on the performance of monolithic DSSC will be analysed in this study by varying the mass ratio of each carbon materials.

## 2. Experimental Methods

### 2.1. Preparation of carbon counter electrode

In this study, glass substrates coated with conductive layer of TEC<sup>TM</sup> 15 (15  $\Omega$  / sq, Dyesol) was used and cut to size of 2 cm  $\times$  1.5 cm. For monolithic configuration, the negative electrode side (photoelectrode) and the positive electrode (counter electrode) of DSSC cells were on the same FTO glass but separated by scribing or removing the FTO layer by using diamond cutter and sandpaper. The substrates were then immersed in deionized water (DI water) mixed with Teepol liquid, and isopropyl alcohol / IPA and cleaned by using Ultrasonic cleaner (Branson 3200) for 10 minutes. The  $\text{TiO}_2$  paste was then printed 2 $\times$  by using screen printing and the substrate was dried in the oven at 120°C for 10 minutes at a time. The  $\text{TiO}_2$  paste used was a commercial paste (Pasta DSL 18 NR-AO, Dyesol). The substrate was subsequently annealed in a furnace at 500°C for 60 minutes [11]. After the annealing process, the samples were immersed in  $\text{TiCl}_4$  (40 mM) solution at 70°C for 30 minutes. The immersion in  $\text{TiCl}_4$  solution served to produce a layer of  $\text{TiO}_2$  reflector that would capture more light [12]. After immersed in  $\text{TiCl}_4$  solution, the substrates were dried in an oven at 120°C for 10 minutes and then annealed in furnace at 500°C. After 60 minutes in the furnace, then  $\text{ZrO}_2$  paste was deposited twice on top of the  $\text{TiO}_2$ . The  $\text{ZrO}_2$  paste used was a commercial paste (Zr-Nanoxide Z / SP, Solaronix). After each deposition, the substrate was dried in oven at 120°C for 10 minutes and then annealed in furnace at 400°C for 60 minutes.

The carbon composite counter electrodes were prepared by using the composition of graphite and amorphous carbon with variation ratio of 4:1 and 1:4. The formulations used in this combination of

materials were based on studies conducted by Zhang et al. using a 1 g carbon black formulation, 4 g of graphite powder, 0.6 g ethyl cellulose, and 8 g terpeneol [7]. In this study, activated carbon and carbon nanopowder were used as a substitute for carbon black [13]. The particle size of this carbon nanopowder was less than 50 nm. The addition of TiO<sub>2</sub> P25 in the formula aimed to avoid cracked films regardless of the substrate [1]. All ingredients were stirred and mixed in a mortar until they were evenly blended in the form of paste. The carbon paste was then deposited on the top of the ZrO<sub>2</sub> layer by using screen printing. The substrate was then dried in the oven at 125°C for 10 minutes to speed up the drying process. After the drying process, the samples were annealed at 400°C in a furnace for 45 minutes.

## 2.2. DSSC Fabrication

All cells were immersed in a dye Z-907 solution (cis-Bis (isothiocyanato) (2,2'-bipyridyl-4,4'-dicarboxylato) (4,4'-di-nonyl-2'-bipyridyl) ruthenium (II), Dyesol), for 24 hours in dark conditions. The samples were subsequently rinsed using ethanol and dried. Then, the cells were sealed by using thermoplastic Surlyn (Dyesol) with a size of 1 mm × 10 mm. The cells were assembled by covering the top layer with a non-conductive glass by using hot press. The Surlyn heating process was conducted for 5 minutes at 120 °C. After the assembly, the electrolyte based I<sup>-</sup>/I<sub>3</sub><sup>-</sup> (EL-HPE, Dyesol) solution was injected in the gap between the two glasses. A silver tab was added prior to the measurement to increase conductivity of the current that flowed to the external circuit [14].

## 2.3. Characterization

The morphology of the carbon layer counter electrode was observed using a 20 kV beam SEM with magnification up to 10,000 times. Using the calculation method of Brunauer, Emmett and Teller (BET) through the gas sorption measurement (Quantachrome Instruments version 11.03), the surface area of the material used as the counter electrode was estimated. The resistivity value of the counter electrode layer was measured using a four-point probe (HP 3468A Multimeter). The crystallinity of the carbon counter electrode was analysed using X-ray diffraction (XRD). The XRD measurement was performed with Cu K $\alpha$  radiation ( $\lambda = 1.54056 \text{ \AA}$ ), 40 kV 30 mA with a range of  $2\theta$  from 10°-90°. The current-voltage characterization (I-V) was carried out using a measurement system from National Instrument with a sun simulator source with AM 1.5 filter and a light intensity of 500 W/m<sup>2</sup> or 0.5 Sun (Oriel, Model: 91192). In addition to I-V characterization, the incident photon-to-current efficiency (IPCE) was also analysed using Newport power meter model 2936-R.

# 3. Results and Discussion

## 3.1. Analysis of physical and electrical characteristics of carbon counter electrode layer

The morphology of the counter electrode layer with several variations of carbon composition is shown in figure 1. Figures 1 (a) and (b) show the SEM images of the counter electrode that uses graphite material (G) and activated carbon (AC), with a ratio of 4:1 (G4:AC1) and 1:4 (G1:AC4). Meanwhile, Figures 1 (c) and (d) are the SEM images of the counter electrode that uses graphite material (G) and carbon nanopowder (CN), with a ratio of 4:1 (G4:CN1) and 1:4 (G1:CN4). All of the counter electrodes are formed as micro-sized agglomerations, with an average size of 1.37  $\mu\text{m}$  and 3.32  $\mu\text{m}$  when using a graphite and active carbon composition with a ratio of 4:1 (G4:AC1) and 1: 4 (G1:AC4), respectively. Meanwhile, the average size of agglomerates is 1.04  $\mu\text{m}$  and 0.83  $\mu\text{m}$  when using composition of graphite and carbon nanopowder with a ratio of 4:1 (G4:CN1) and 1:4 (G1:CN4), respectively. It can also be observed that the graphite and active carbon composition with a ratio of 1:4 (G1:AC4) have larger gaps between the agglomerates as indicated by the darker areas. The larger gap is affected by the size of the resulting agglomerates. The darker areas indicate that the resulting composite is more porous [14]. Thus, the graphite and active carbon composition with a ratio of 1:4 (G1:AC4) result in a more porous counter electrode layer than the other compositions.

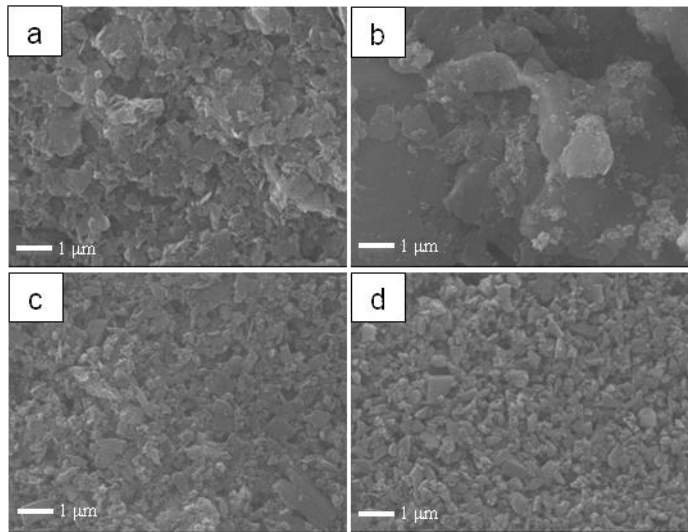


**Figure 1.** SEM results on morphology of carbon counter electrode layer with variation composition of graphite (G) and active carbon (AC) (a) G4:AC1; (b) G1:AC4, and composition of graphite (G) and carbon nanopowder (CN) (c) G4:CN1; (d) G1:CN4.

Through the BET method, a wide range of surface area is obtained with a variety of carbon compositions. The BET surface area when using graphite and active carbon composition with a ratio of 4:1 (G4:AC1) and 1:4 (G1:AC4) is 54.22 m<sup>2</sup>/g and 37.93 m<sup>2</sup>/g, respectively. Meanwhile the surface area when using composition of graphite and carbon nanopowder with a ratio of 4:1 (G4:CN1) and 1:4 (G1:CN4), which is 49.40 m<sup>2</sup>/g and 79.80 m<sup>2</sup>/g.

Counter electrodes ideally shall have high conductivity to improve the photovoltaic performance [3].

From the four-point probe measurements, the average resistivity value of the counter electrode layer using composition of graphite and active carbon with a ratio of 4:1 (G4:AC1) and 1:4 (G1:AC4) is 11.95 Ω/sq and 11.60 Ω/sq, respectively. Meanwhile, the resistivity is 12.39 Ω/sq and 12.44 Ω/sq when graphite and carbon nanopowder with a ratio of 4:1 (G4:CN1) and 1:4 (G1:CN4) are used, respectively. From these data it can be observed that the lowest resistivity value is achieved when using composition of graphite and active carbon with a ratio of 1:4.

The result of XRD characterization is shown in figure 2. The graphite peaks are identified based on COD 96-901-2231 data, while the TiO<sub>2</sub> anatase and rutile phases are identified based on data ICSD 98-004-4882 and ICSD 98-016-9638, respectively. In figure 2 (a), it can be observed that the graphite material has a high peak and taper. The strong peak indicates that graphite has high crystallinity [1]. Figures 2 (b) and (c) show the XRD results after graphite has been combined with carbon nanopowder. TiO<sub>2</sub> anatase and rutile phases appear in both figures. After graphite was combined with carbon nanopowder, there is a decrease in the graphite crystallinity. This is because the amorphous carbon material has a low crystallinity and the particles are small and do not have perfect order [15]. Thus, when amorphous carbon and graphite materials are combined, the particles connection between graphite is stronger. This is because graphite has larger particle size, which means there are plenty of free spaces to be filled by the amorphous carbon materials [1].

### 3.2. Performance analysis of DSSC monolithic

Material composition at the counter electrode layers can affect the monolithic DSSC performance. The I-V characterization results and curves with variations in the carbon compositions are shown in table 1 and figure 3, respectively.

Photovoltaic performance generated in solar cells can be affected by short-circuit current,  $I_{sc}$ . Based on the I-V data in table 1, the highest  $I_{sc}$  value generated when using composition of graphite and activated carbon with a ratio of 1: 4 (G1:AC4), which is 1.19 mA. This is because  $I_{sc}$  affected by the porosity of counter electrode, which can have an effect on the dye absorption [14]. Based on figure 1 (b), the SEM image of graphite with activated carbon with a ratio of 1:4 is more porous compared to composition of graphite and carbon nanopowder.

The highest efficiency, i.e. 1.52%, is achieved when using graphite and activated carbon composition as a counter electrode with a ratio of 1: 4. The efficiency of DSSC is influenced by the  $I_{sc}$  value [4]. Based on table 1, the highest  $I_{sc}$  values generated when the composition has fewer graphite ratios compared to activated carbon. Overall, the values of the fill factor (FF) produced are relatively low ( $<0.5$ ). The resulting FF can be affected by the resistance value in the monolithic DSSC. Based on table 1, the resulting resistance value is relatively high. A high resistance value can lower the FF, thus degrading the performance of the monolithic DSSC [16].

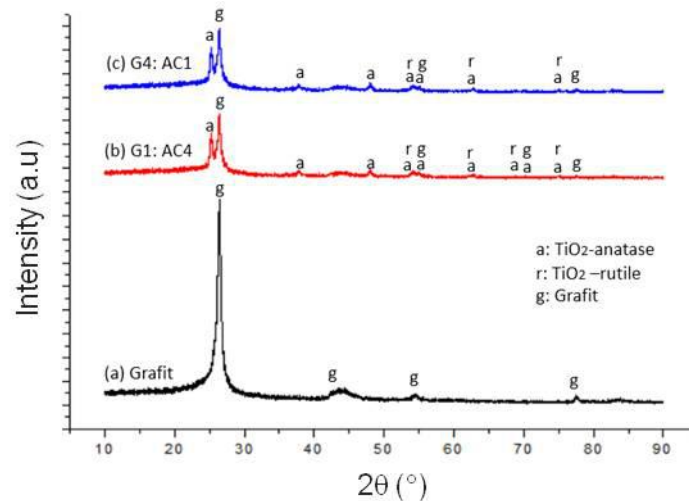


**Figure 2.** XRD spectra of the carbon counter electrode material.

**Table 1.** Photovoltaic characteristics in monolithic DSSC with carbon composition variation for the counter electrodes.

Ratio	$I_{sc}$ (mA)	$V_{oc}$ (V)	$P_{max}$ (mW)	FF	$R_s$ (k $\Omega$ )	$R_{sh}$ (k $\Omega$ )	Eff. (%)
G4:AC1	0.81	0.61	0.13	0.25	0.79	0.72	0.99
G1:AC4	1.19	0.63	0.19	0.25	0.53	0.52	1.52
G4:CN1	0.10	0.49	0.02	0.29	28.25	4.82	0.12
G1:CN4	0.06	0.53	0.01	0.27	6.88	8.50	0.07

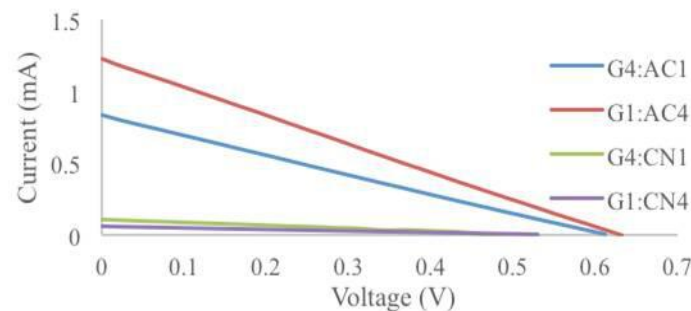


**Figure 3.** I-V curves of monolithic DSSC with material composition variations in the counter electrode.

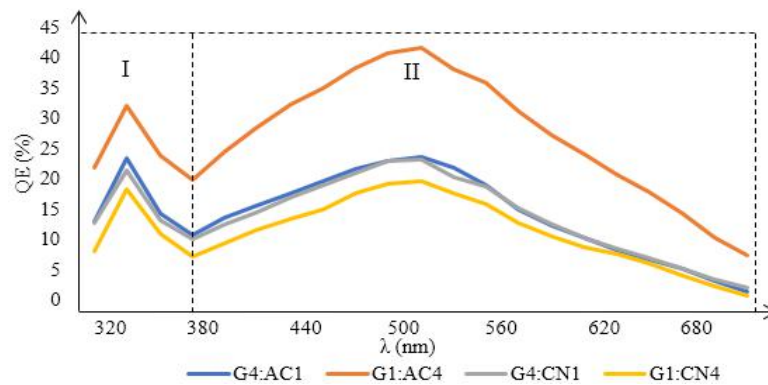


**Figure 4.** IPCE graph with material composition variations in the counter electrode.

IPCE measurement is conducted to analyse the quantum efficiency (QE), which is the ratio between the amounts of charge that contributes in generating current to the number of photons provided. The QE spectra are shown in figure 4. Figure 4 indicates that the resulting light absorption area is in the UV and visible light range, i.e. 320 - 720 nm. There are two peaks produced, which is in the absorption area of  $\text{TiO}_2$  that is shown in region I and the dye absorption region Z907 that is shown in region II.

In the absorption area of  $\text{TiO}_2$ , a high QE value of 32% is obtained at 340 nm when using graphite composition and activated carbon as a counter electrode with a ratio of 1:4 (G1:AC4). The peak in the wavelength area of 520 nm is the peak absorption area of the Z907 dye. Similar to the  $\text{TiO}_2$  absorption area, high QE value in the Z907 dye absorption area is obtained when using graphite and activated carbon at a ratio of 1:4 (G1:AC4). The high QE value suggests that the counter electrode is able to flow the dye well so that the dye can enter and be adsorbed more by the photoelectrode [14]. With maximum dye absorption, a high  $I_{sc}$  value can be obtained. Thus,  $I_{sc}$  can affect the QE values generated in DSSC [3]. Figure 4 also shows that the absorption area of  $\text{TiO}_2$  and dye Z907 do not have much different QE values between the G4:AC1 sample and the G4:CN1 sample. However, Table 1 shows that the  $I_{sc}$  values are significantly different for both samples. The reason for this can be due to poor contact as indicated by the  $R_s$  value produced [16]. Based on table 1, it can be observed that the  $R_s$  value for the G4:AC1 sample and the G4:CN1 sample differs greatly.

#### 4. Conclusions

In this study, we conclude that the carbon materials composition on the electrode counter can significantly affect the performance of the monolithic DSSC. Different types of carbon produce different physical and electrical characteristics on the counting electrode, i.e. different porosity, crystallinity, surface area, and particle size, but relatively similar conductivity values. The results of this study show that the best composition is achieved by the combination of graphite and activated carbon with a ratio of 1: 4 that yield a porous layer, with the size of 3.32  $\mu\text{m}$  agglomerates, and the sheet resistance of 11.60  $\Omega/\text{sq}$ . The highest resulting efficiency is 1.52% and the highest QE value is 32% at absorption area of  $\text{TiO}_2$ , with values of  $V_{oc}$ ,  $I_{sc}$  and  $P_{max}$  respectively being 0.63 V, 1.19 mA and 0.91 mW.

#### Acknowledgements

This research was funded by the INSINAS research program 2017-2018 by the Ministry of Research, Technology and Higher Education (Kemristekdikti) entitled "Rancang, Bangun dan Upscaling Modul Surya Berbasis Warna dengan Struktur Monolitik untuk Aplikasi Penghasil Listrik Indoor". The authors would like to thank the Materials and Devices for Solar Cells research group at the Telecommunication and Telecommunication Research Center - Indonesian Institute of Sciences



(P2ET-LIPI) at Bandung and Surya University for their support. Research Center for Physics (P2F-LIPI) and Research Unit for Clean Technology (LPTB-LIPI) is gratefully acknowledged for conducting the XRD and SEM, respectively. F. Arif and N. M. Nursam contributed equally to this work.

## References

- [1] Ito S and Takahashi K 2012 *Int. J. Photoenergy* **2012** 1
- [2] Vesce L, Riccitelli R, Mincuzzi G, Orabona A, Soscia G, Brown T M, Di Carlo A, and Reale A 2013 *IEEE J. Photovoltaic* **3** 1004
- [3] Wu J, Lan Z, Lin J, Huang M, Huang Y, Fan L, Lou G, Lin Y, Xie Y, and Wei Y, 2017 *Royal Soc. Chem.* **46** 5975
- [4] Wu M, and Ma T 2014 *J. Phys. Chem.* **118** 16727
- [5] Thomas S, Deepak T G, Anjusree G S, Arun T A, Nair S V, and Nair A S 2014 *J. Mater. Chem. A* **2** 4474
- [6] Veerappan G, Bojan K, and Rhee S-W 2011 *ACS Appl. Mater. Interfaces* **3** 857
- [7] Zhang J, Meng Z, Gou D, Zou H, Yu J, and Fan K 2018 *Appl. Surf. Sci.* **430** 531
- [8] Burnside S, Winkel S, Brooks K, Shklover V, Gratzel M, Hinsch A, Kinderman R, Bradbury C, Hagfeldt A, and Petterson H 2000 *J. Mater. Sci.: Mater. Electronic* **11** 355
- [9] Chen J, Li K, Lou Y, Gou X, Li D, Deng M, Huang S, and Meng Q 2009 *Carbon* **26** 2704
- [10] Lim J, Ryu S Y, Kim J, and Jun Y 2013 *Nanoscale Res. Lett.* **8** 227
- [11] Nursam N M, Anggraini P N, Shobih, and Hidayat J 2017 *International Conference on Radar, Antenna, Microwave, Electronics, and Telecommunications (ICRAMET) 2017*
- [12] Rho W, Chun M, Kim H, Hahn Y, Suh J S, and Jun B 2014 *Bull. Korean Chem. Soc.* **35** 1165
- [13] Ito S and Mikami Y 2011 *Pure Appl. Chem* **83** 2089
- [14] Nursam N M, Istiqomah A, Hidayat J, Anggraini P N, and Shobih 2017 *J. Elektronika dan Telekomunikasi* **17** 30
- [15] Hornyak G L, Tibbals H F, Dutta J and Moore J J 2008 *Introduction to nanoscience and nanotechnology* Boca Raton: CRC Press
- [16] Mertens K 2014 *Photovoltaics fundamental, technology and practice* Wiley: Germany